Characteristics of RSSI Kriging Interpolated Value in Neighborhood of Buildings

Ryo Miyamoto*, Shusuke Narieda†, Takeo Fujii‡ and Hiroshi Naruse†
*Dept. Inform Eng., Faculty of Eng., Mie University, Tsu, Mie, Japan.
†Dept. Inform Eng., Graduate School Eng., Mie University, Tsu, Mie, Japan.
‡Advance Wireless Communication Research Center, Univ. Electro-Commun., Chofu, Tokyo, Japan.
E-mail: narieda@pa.info.mie-u.ac.jp

***Abstract*—This study investigates the effect of buildings on the accuracy of Kriging interpolation result for estimating for the received signal strength indicator (RSSI) in the sub-GHz band. The RSSI values can be estimated using Kriging interpolation, which is an interpolation method and that depends on the distance and shadowing components. Traditionally, the accuracy of estimation by Kriging interpolation in the neighborhood of a building has never been verified. In this study, analyses of the accuracy of Kriging interpolation in the neighborhood of a building are provided by comparing the actual observed RSSI values with the values estimated by Kriging interpolation. This study verifies that the estimation accuracy can be improved by changing the area where the observations used for Kriging interpolation are obtained and by increasing the number of observations used for interpolation, even in the neighborhood of buildings. In addition, estimation accuracy can be improved by obtaining the observed value from the area near the interpolated location.**

I. Introduction

In recent years, the concept of the Internet of Things (IoT) has attracted attention. Many IoT devices with wireless transceivers and physical sensors are geographically deployed to gather information, and they are utilized in various applications, such as smart city applications [1], human centric health and wellness monitoring applications [2], and environmental monitoring [3]. Such applications can be realized to construct wireless sensor networks composed of many IoT devices and gateways. Because IoT devices are battery-powered, low power consumption is expected for these IoT devices. Low-Power Wide-Area networks (LPWANs) [4] operating in the sub-GHz band are capable of long-range communications and battery efficiency, and low-power wide-area (LPWA) technology can be expected to serve as a communication infrastructure for such IoT systems.

The IoT devices are deployed according to the requirements of each IoT system and radiowave propagation information, which can be obtained from a two-dimensional radio environment map [5]. The radio wave propagation of LPWA technology in the sub-GHz band has been investigated [6]. In their experiment, the propagation on the road in the university campus is measured for the analysis, and the propagation is modeled based on the measurement result. However, although the road is easily accessible, the IoT devices are usually placed in areas that are inaccessible to humans, such as areas in the implantation, where it is difficult to pre-measure the received signal strength indicator (RSSI). In other words, they are less likely to be placed in the path of humans to avoid getting in the way. The RSSI in such areas can be estimated using Kriging interpolation [7]. Kriging interpolation is an interpolation method that depends on distance and shadowing component. The accuracy of the RSSI value estimated by Kriging interpolation in the neighborhood of buildings has never been verified.

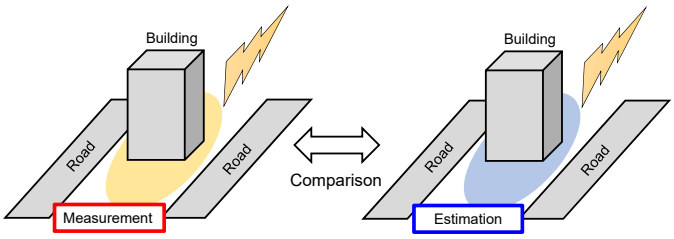

Fig. 1. Overview of this study: comparison of measured and estimated RSSI values in the neighborhood of buildings.

In this study, we investigate the effect of buildings on the accuracy of Kriging interpolation for estimating the RSSI in the sub-GHz band. Fig. 1 presents an overview of the study. The RSSI value obtained using Kriging interpolation is compared with the actual observed RSSI on the road around the buildings are obtained by actual observation, and the estimated values of the RSSI in the neighborhood of the buildings are calculated by Kriging interpolation. The accuracy of Kriging interpolation in the neighborhood of the buildings is verified by comparing the actually observed RSSI with the estimated value.

II. Kriging Interpolation

A. RSSI interpolation model

The radio environment map can be constructed by actually observing the received signal power. However, since it is difficult to obtain the measured RSSI in the inaccessible area, the map can be obtained using Kriging interpolation. The interpolation value $\widehat{P}(\mathbf{x}_0)$ of the average received signal power can be written as

$$\widehat{P}(\mathbf{x}_0) = \widehat{P}_C - 10\widehat{\eta}\log_{10}\|\mathbf{x}_0 - \mathbf{x}_{T_x}\| + \widehat{W}(\mathbf{x}_0) \quad (1)$$

where $\mathbf{x}_0$ and $\mathbf{x}_{T_x}$ are the position coordinate vector to be estimated and position coordinate vector of the transmitter, respectively. Furthermore, $\widehat{W}(\mathbf{x}_0)$ is the estimated value of the shadowing component, and $\widehat{P}_C$ and $\widehat{\eta}$ are the values corresponding to b and a, respectively, in the least squares method $y = ap(x) + b$.

B. Interpolation method

In Kriging interpolation, the estimate can be obtained from the observed RSSI and its geographical position information, and it is well known to be effective in estimating the shadowing components. The estimate obtained from Kriging interpolation is given by

$$\widehat{W}(x_0) = \sum_{i=1}^{N} w_i \widehat{W}(x_i) \tag{2}$$

where $\widehat{W}(\mathbf{x}_0)$, $\widehat{W}(\mathbf{x}_0)$, N, and w_i are the estimate of the shadowing component at the point of interest, the ith estimate of the shadowing component obtained from the observed RSSI using the least square method, the number of observed RSSI values, and the ith weight coefficient, respectively. In Kriging interpolation, the weighting factors are optimized by minimizing the variance $\sigma_k^2 = \mathrm{Var}\left[Z(\mathbf{x}_0) - \widehat{Z}(\mathbf{x}_0)\right]$ of the error under the condition $\sum_{i=1}^{N} w_i = 1$, as a constraint on unbiasedness. Using these equations and the Lagrange multiplier μ, the objective function can be expressed as $\phi(w_i, \mu) = \sigma_k^2 - 2\mu\left(\sum w_i - 1\right)$ where σ_k^2 can be written as [7]

$$\sigma_k^2 = -\gamma(d_{0,0}) - \sum_{i=1}^{N}\sum_{j=1}^{N} w_i w_j \gamma(d_{i,j}) + 2\sum_{i=1}^{N} w_i \gamma(d_{i,0}), \tag{3}$$

where $\gamma(\cdot)$ is a semivariogram that satisfies $\gamma(\|\mathbf{x}_i - \mathbf{x}_j\|) = \mathrm{Var}[f]/2$, and $\|\mathbf{x}_i - \mathbf{x}_j\| \equiv d_{i,j}$. In this study, the empirical semivariogram can be approximated by a theoretical semivariogram as the exponential model, which is given by

$$\gamma(d) = \alpha_n^2 + \alpha_s^2 \left\{1 - \exp\left(-\frac{d}{\alpha_r}\right)\right\}, \tag{4}$$

where d, α_n^2, α_s^2, and α_r are the distance between the ith point and the jth point, nugget, sill and range, respectively. Furthermore, α_n^2, α_s^2, and α_r are parameters of the semivariogram. By partially differentiating the objective function by each weighting factor and setting the result to zero, the following simultaneous equations of $N+1$ elements are obtained,

$$\begin{bmatrix} \gamma(d_{1,1}) & \cdots & \gamma(d_{1,N}) & 1 \\ \vdots & \vdots & \vdots & \vdots \\ \gamma(d_{N,1}) & \cdots & \gamma(d_{N,N}) & 1 \\ 1 & \cdots & 1 & 0 \end{bmatrix} \begin{bmatrix} w_1 \\ \vdots \\ w_N \\ \mu \end{bmatrix} = \begin{bmatrix} \gamma(d_{1,0}) \\ \vdots \\ \gamma(d_{N,0}) \\ 1 \end{bmatrix}. \tag{5}$$

By solving the simultaneous equation, w_i, that minimizes σ_k^2 can be obtained. Using w_i, $\widehat{W}(\mathbf{x}_0)$ can be estimated.

III. Experimental Analysis

A. Experiment Setup

To verify the estimation accuracy of the RSSI using Kriging interpolation in the neighborhood of buildings, the actual observed RSSI values are compared with the estimated values. Specifically, the observed RSSI and the estimates are compared for each divided area according to whether the library affects radio wave propagation. We employ LoRaWAN [8] as the LPWAN in the experiment. Fig. 2 shows a LoRa transmitter and LoRa receiver. The LoRa transmitter is composed of a LoRa module and a laptop for controlling the module, and it is installed on the rooftop of a five-story reinforced concrete building at Mie University. The LoRa receiver is composed of a LoRa module, battery, global navigation satellite system (GNSS) receiver, Raspberry PI3 B+, and a small display. During the experiment, the LoRa receiver measures the RSSI around the library as shown in Fig. 3, and acquires the geographical position information of the measurement point. Furthermore, the transmission time interval, transmission power, center frequency, spreading factor, and bandwidth are set to 1 sec, 13 dBm, 923.2 MHz, 7, and 125 kHz, respectively.

B. Experiment Results

The measurements are executed in the area indicated by the color scale shown in the lower part of the figure. In Fig. 3, area A is the area where the observation is affected by the library, area C is the area where the observation is not affected by the library, and area B is the union of areas A and C, that is, $B = A \cup C$. Area C is divided into areas C_1, C_2, and C_3, that is, $C = C_1 \cup C_2 \cup C_3$. Based on the measurement results in each area, the estimate of the RSSI in an evaluation area around the library shown in Fig. 3 is obtained using Kriging interpolation. Table I shows the root mean square error (RMSE) results for each observation area and the estimates. The RMSE is defined by,

$$\mathrm{RMSE} = \sqrt{\frac{1}{n}\sum_{i=1}^{n}(x_i - \hat{x}_i)^2} \tag{6}$$

From Table I, the RMSE of the comparison results in area B is superior to that in other areas. It can be seen that the estimation accuracy can be improved by increasing the number of observations used for interpolation, even in the neighborhood of buildings. Furthermore, it can be seen that the estimation accuracy can be improved by obtaining the observed value from the area close to the interpolated location.

TABLE I
Comparison result of RMSE between measurement and Kriging interpolated results.

	A	B	C	C_1	C_2	C_3
Number of observations	185	332	295	54	134	107
RMSE [dB]	2.34	2.28	3.94	6.64	3.95	8.85

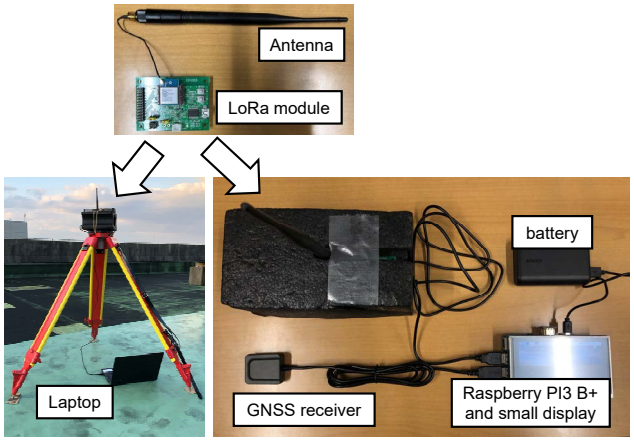

Fig. 2. LoRa transmitter (left-hand side) and LoRa receiver (right-hand side).

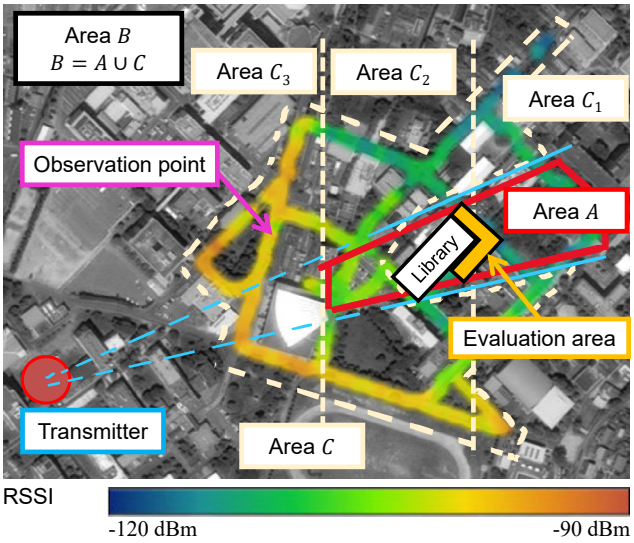

Fig. 3. Actual measurement results in three areas, area A, area B, area C, area C_1, area C_2, and area C_3. $B = A \cup C$ and $C = C_1 \cup C_2 \cup C_3$.

Finally, we present the distribution of RMSE in the neighborhood of the library for each area where the observed data were obtained. Fig. 4 shows the distribution of RMSE. In Fig. 4, the RMSEs around the library are represented by the colors shown in the lower part of the figure, which are normalized using the maximum and minimum values in each area. Although the accuracy of Kriging interpolation in each area is different as shown in Table I, a tendency for the distribution of the RMSE is similar to each other.

IV. Conclusion

This study investigated the accuracy of Kriging interpolation for estimating RSSI in the neighborhood of buildings. In the study, the observed RSSI value and the RSSI value estimated by Kriging interpolation were compared and verified using the RMSE metric. This study demonstrates that the estimation accuracy can be improved by changing the area where observation values used for Kriging interpolation are obtained and

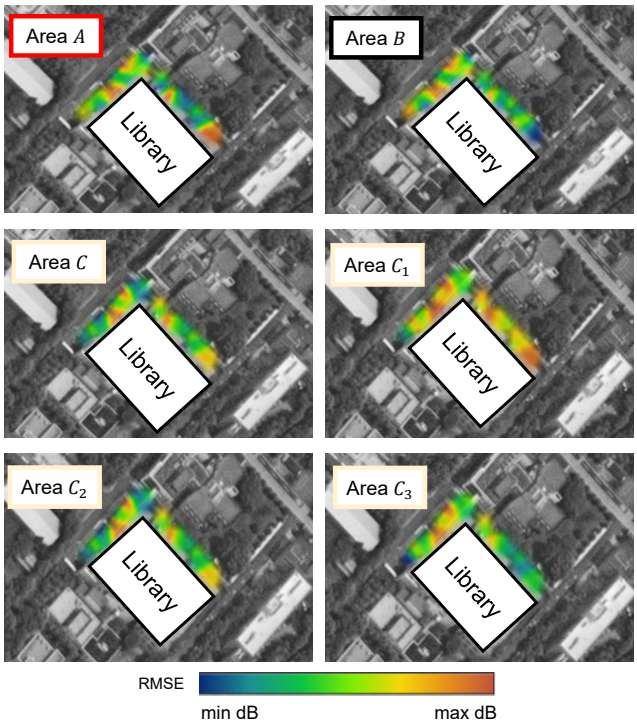

Fig. 4. Distributions of RMSE at neighborhood of library for each area where observed data were obtained.

increasing the number of observation values used for interpolation, even in the neighborhood of buildings. Furthermore, the estimation accuracy could be improved by obtaining the observed value from the area near the interpolated location.

Acknowledgement

This research and development work was supported by the MIC/SCOPE #JP215006001.

References

[1] D. Magrin, M. Centenaro, and L. Vangelista, "Performance Evaluation of LoRa Networks in A Smart City Scenario," in *Proceeding of the 2017 IEEE International Conference on Communications (ICC)*, 2017, pp. 1–6.
[2] J. Petäjäjärvi, K. Mikhaylov, M. Hämäläinen, and J. Iinatti, "Evaluation of LoRa LPWAN Technology for Remote Health and Wellbeing Monitoring," in *Proceeding of the 2016 10th International Symposium on Medical Information and Communication Technology (ISMICT)*, Mar. 2016, pp. 1–5.
[3] L. Joris, F. Dupont, P. Laurent, P. Bellier, S. Stoukatch, and J. Redoute, "An Autonomous Sigfox Wireless Sensor Node for Environmental Monitoring," *IEEE Sensors Letters*, vol. 3, no. 7, pp. 01–04, 2019.
[4] U. Raza, P. Kulkami, and M. Sooriyabandara, "Low Power Wide Area Networks: An Overview," *IEEE Commun. Surveys Tuts.*, vol. 19, no. 2, pp. 855–873, Secondquater 2017.
[5] H. B. Yilmaz, T. Tugcu, F. Alagöz, and S. Bayhan, "Radio Environment Map as Enabler for Practical Cognitive Radio Networks," *IEEE Communications Magazine*, vol. 51, no. 12, pp. 162–169, 2013.
[6] K. Inagaki, S. Narieda, T. Fujii, K. Umebayashi, and H. Naruse, "Measurements of LoRa Propagation in Harsh Environment: Numerous NLOS Areas and Ill-Conditioned LoRa Gateway," in *2019 IEEE 90th Vehicular Technology Conference (VTC2019-Fall)*, 2019, pp. 1–5.
[7] N. Cressie, *Statistics for Spatial Data*. Wiley-Interscience, 1993.
[8] https://lora-alliance.org/.